Solvation of N_3^- at the Water Surface: The Polarizable Continuum Model Approach

Laban Bondesson,[†] Luca Frediani,*[,‡] Hans Ågren,[†] and Benedetta Mennucci[§]

Laboratory of Theoretical Chemistry, AlbaNova University Center, Royal Institute of Technology, S-10691 Stockholm, Sweden, Department of Chemistry, University of Tromsø, N-9037 Tromsø, Norway, and Dipartimento di Chimica e Chimica Industriale, Università di Pisa, Via Risorgimento 35, 56126 Pisa, Italy

Received: February 7, 2006; In Final Form: April 3, 2006

We present a new quantum mechanical model to introduce Pauli repulsion interaction between a molecular solute and the surrounding solvent in the framework of the Polarizable Continuum Model. The new expression is derived in a way to allow naturally for a position-dependent solvent density. This development makes it possible to employ the derived expression for the calculation of molecular properties at the interface between two different dielectrics. The new formulation has been tested on the azide anion (N_3^-) for which we have calculated the solvation energy, the dipole moment, and the static polarizability at the interface as a function of the ion position. The calculations have been carried out for different ion−surface orientations, and the results have also been compared with the parallel electrostatic-only solvation model.

1. Introduction

Understanding ion behavior at the gas/liquid interface is of fundamental importance in a wide variety of problems, from environmental pollution to the structure and stability of large biomolecules and membranes or the transport of ions through ion channels in cellular membranes, just to quote a few examples.

Despite this fundamental importance, characterization of the interfaces at the molecular level is rather limited both theoretically and experimentally. Only recently, advances in modern instrumentation and in theoretical and computational models have significantly improved this situation (see, for example, the very recent reviews by Chang and Dang[1] and Jungwirth and Tobias[2] for a complete literature). On the experimental side, techniques, such as nonlinear optical spectroscopy, X-ray diffraction and reflection, and neutron reflection, have allowed the measuring of molecular details at the interface. On the theoretical side, most developments have been obtained with molecular simulation approaches, such as molecular dynamics (MD) and Monte Carlo (MC) techniques.

In particular, most of the simulation and experimental works have focused on one essential question regarding solvation at an interface, namely, the details of ion distributions. Despite the apparent simplicity, this key issue has, in fact, remained elusive until very recently.

The traditional view was that ions were repelled from interfaces. This picture was derived from surface tension measurements and was theoretically explained by Wagner[3] using the Debye−Huckel theory of electrolytes. According to his study, because of the variation in the dielectric constants across the interface, the presence of ions at the interface induces image surface charges that have the same magnitude and sign. Such image charges repel the ions from the surface and thus reduce the concentrations of ions at the interface. The surface tension accordingly increases on addition of a simple electrolyte. Such a theory was further developed by Onsager and Samaras,[4] who obtained an analytical limiting law of the salt effect on surface tension.

This picture was confirmed by standard MD simulations until the introduction of polarizable potentials showed that while small, nonpolarizable (hard) ions (e.g., alkali cations and fluoride anions) are repelled from the interface by the electrostatic image forces, larger polarizable (soft) ions, such as the heavier halides, nitrate, or azide, exhibit an enhancement in their surface concentrations.[5−12]

This new conclusion obtained by calculations has also been reached by the results of second harmonic generation (SHG) or sum frequency generation (SFG) experiments on the surfaces of aqueous salt solutions as well as the surfaces of aqueous acids and bases.[13−15]

Such important developments in the understanding of the ion behavior at interfaces have led to a renewed interest in the application of quantum mechanical continuum models to the same problem. An example of this trend is represented by the recent extensions of the Integral Equation Formalism (IEF) version[16−18] of the Polarizable Continuum Model (PCM)[19] to the study of atomic and molecular solutes at gas−liquid and liquid−liquid interfaces.[20−22] Within this framework, the interface is modeled in terms of macroscopic properties (e.g., density and permittivity) varying smoothly in the interfacial region. The model allows the inclusion of both electrostatic and repulsion effects arising from this inhomogeneous environment into the quantum chemical calculation on the solute.

In particular, such a model has been applied to a study of static polarizabilities of halides (fluoride, chloride, bromide, and iodide) at the water/air interface.[22] This property has then been connected to other relevant quantities, such as the free energy profiles and the dipole moment, to explain the observed interfacial preference of the heavier halides. A result of that study concerned the role of the various physical interactions that concur in determining the behavior of the heavier halides. As previously expressed, MD works attribute the polarizability to the role of yielding the halides' surface preference, where, instead, the comparison of two different continuum models (electrostatic-only and electrostatic + repulsion) seems to

* Corresponding author. E-mail: luca@chem.uit.no.
[†] Royal Institute of Technology.
[‡] University of Tromsø.
[§] Università di Pisa.

10.1021/jp060794p CCC: $33.50
Published on Web 05/24/2006

indicate that there exists a more complex situation in which polarization and repulsion effects combine to give the observed interfacial preference of the heavier halides.

Here we extend the model to a more complex solute (the azide N_3^- ion) for which femtosecond second harmonic generation (SHG) experiments[13] and measurements of photoelectron spectroscopy[23] have shown an enhanced concentration at the gas−water surface. As in the reference paper, also here we analyze the relative importance of electrostatic and repulsion solute−solvent interactions between the solute species and the solvent to determine the interface behavior of the azide ion by using the IEF−PCM approach. The lack of spherical symmetry of this solute, however, has required a reformulation of the QM model for the repulsion interactions with respect to that used in the reference paper.[22]

2. The Theoretical Model

In this section, we will first briefly review the theoretical background of the IEF−PCM, emphasizing the aspects which are relevant for the present study, namely, the extension to liquid surfaces and interfaces and the modeling of the repulsion contribution. This last aspect will be dealt with in more detail since the present work required a further development of the model in order to be able to handle the problem under investigation.

2.1. The Basic Assumption in Continuum Models. The general idea of a continuum solvation model is to take into account the interaction between the molecular solute and the surrounding solvent by reproducing it as an effective field acting on the solute.[24,25] The molecule is treated as if it was an isolated system, where the Hamiltonian of the system, H_{eff}, contains, in addition to the gas-phase Hamiltonian H_0 (kinetic energy, potential energy, and electronic repulsion), also those terms, grouped here as V_{int}, describing the solute−solvent interaction:

$$H_{\text{eff}} = H_0 + V_{\text{int}} \tag{1}$$

Since the founding of solvation theory with the Onsager model,[26] the solute−solvent interaction V_{int} was limited to the electrostatic forces between a homogeneous solvent and the solute immersed in it. Such models are now mature, and the electrostatic interaction is—in principle—reproduced exactly for cavities of arbitrary shape.[25] The success of the model led to further developments in several directions. Two of these are considered in the present study: on the one side, the attempt to extend the model to different environments besides the homogeneous isotropic dielectric representing the bulk of a solution; on the other side, the attempt to introduce in the model other solute−solvent interactions between the solute and the solvent.

2.2. Electrostatics at Liquid Interfaces: The IEF−PCM Approach. The extension of the PCM to interfaces between two different dielectrics is based on the assumption that the environment can be treated as a dielectric medium with smoothly varying, position-dependent properties along the direction perpendicular to the interface. The only formal constraint is that, at long distances from the interface, the bulk properties of the two media are recovered: no other assumption on the shape of the profile is made. In practice, given a macroscopic property, f, its variation at the interface $f(z)$ is assumed to have a sigmoidal shape, as shown in Figure 1.

To describe the electrostatic interaction of a molecular solute immersed in a dielectric in the framework of the IEF−PCM, it is sufficient to compute Green's function of the problem on the cavity surface $G(x, y)$. For a planar interface, the formal

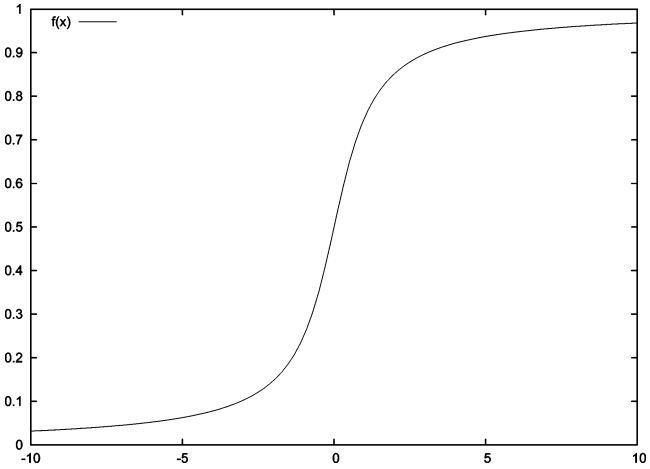

Figure 1. General shape ($f(x) = \text{atan}(x)/\pi + 1/2$) employed to describe variation of properties at the interface. The function is translated/dilated in the x direction (distance) to match position and width of the interface, and in the y direction (medium property) to match the bulk values at $x = \pm\infty$.

derivation of $G(x, y)$ was determined in the 70s[27−29] and was very recently re-casted in a Boundary Element Method (BEM) scheme.[21] The details of the derivation can be found in the above cited papers. It is worthwhile mentioning here that such a Green's function cannot be expressed in a closed form, but a numerical integration must be employed for all required x, y values. In the IEF−PCM approach, they correspond to all possible pairs of representative points x_i and y_i of the discretized cavity surface. Formally, the expression of $G(x, y)$ is the following:

$$G_{\text{E}}(x, y) = \frac{1}{D(\epsilon(z))|x - y|} + G_{\text{E}}^{\text{img}}(x, y) \tag{2}$$

In the equation above, the first term represents a Coulomb-like interaction corresponding to a homogeneous environment having a dielectric permittivity D which depends on the permittivity profile at the interface. The second term, by analogy with a sharp planar interface, represents an image−charge interaction. For a generic interface profile described by a permittivity $\epsilon(z)$, $G_{\text{E}}(x, y)$ is obtained by a numerical integration. For further details on the derivation and its implementation, see ref 21.

With this approach the electrostatic problem for planar interfaces of arbitrary profile is—in principle—solved exactly, with the only approximation being connected to the BEM approach to formulate the problem in a discrete, solvable form.

2.3. Reformulation of the Repulsion Problem. The calculation of the repulsion interaction in the PCM is based upon the theory of weak intermolecular interactions, where the repulsion energy accounts for the Pauli repulsion of the electronic densities of the two separate subsystems.[30,31]

Its extension to a solute−solvent system described within the PCM has been done by assuming that the fraction of the solute electronic density, which is lying outside the cavity (any molecular electronic density vanishes only at infinite distance), will interact with the electron density of the solvent molecules. Since the solvent wave function is not known, a uniform electron density proportional to the number of valence electrons of the solvent, $n_{\text{val}}^{\text{B}}$, and to the solvent number density, ρ_{B}, is assumed.[32] Within such a framework, the repulsion free energy can be written as follows:

$$G_{\text{rep}} = \alpha \int_{r \notin C} \mathrm{d}r P(\mathbf{r}) \tag{3}$$

where C is the solute cavity domain, $P(\boldsymbol{r})$ is the solute molecular density, and $\alpha = 0.063\ \rho_B n_{val}^B/M_B$, where M_B is the solvent molecular weight. Equation 3 shows the direct dependence of the repulsion free energy on the fraction of the solute electronic density lying outside the cavity (the integral is, in fact, on the whole volume excluding the cavity domain). Such an integral can alternatively be expressed as the difference between the total number of electrons and the electrons really inside the cavity. This alternative form of eq 3 can then be used to obtain the corresponding quantum mechanical operator to be added to the electrostatic one in the solute−solvent interaction V_{int} of eq 1. In fact, by formally differentiating with respect to the density matrix, P, the repulsion interaction Hamiltonian becomes

$$h_{rep} = \frac{\delta G_{rep}}{\delta \boldsymbol{P}} = \alpha[\boldsymbol{S} - \boldsymbol{S}^{(in)}] \tag{4}$$

where $\boldsymbol{S}$ is the overlap matrix and $\boldsymbol{S}^{(in)}$ involves a sum of electric field integrals on the cavity surface (the details of the derivation as well as the exact form of all the terms can be found in ref 32).

Such an expression for h_{rep} is well suited for homogeneous solvents but not for interfaces since it is derived assuming a uniform solvent density, ρ_B, which is in fact factored out of the integration of eq 3 and included in the numerical prefactor α. Its straightforward and heuristic extension to the interface has been successfully employed in a previous work,[22] but in that case, all solutes (halogen ions) were characterized by a spherical cavity. The same approach has been found to be inadequate for treating molecular systems of general shape and symmetry; therefore, a different approach has been developed here. The starting point is once again the expression for the repulsion free energy as in eq 3.

Let us start by considering the case of a spherically symmetric solute placed in the center of a spherical cavity with radius R and having an electron density $P(r)$ depending only on the distance from the origin r. Since Gaussian basis sets are generally employed, we will also assume that outside the solute cavity we could model the density as

$$P(r) \simeq P(R)\frac{e^{-\beta r^2}}{e^{-\beta R^2}} \tag{5}$$

No assumption is made for the density inside the molecular cavity. The value of the constant β is obtained by noticing that by integrating eq 5 outside the cavity the number of outlying electrons, n_{out}, must be obtained. Since n_{out} can alternatively be computed by the Gauss theorem on the spherical cavity, then the parameter β is determined unambiguously as

$$n_{out} = P(R)\int_{r\notin C} \mathrm{d}\boldsymbol{r}\, \frac{e^{-\beta r^2}}{e^{-\beta R^2}} \tag{6}$$

If one relaxes the assumption of a constant density at the cavity surface, but maintains the radial decay as in eq 5, eq 6 has then to be rewritten as follows:

$$n_{out} = \frac{1}{e^{-\beta R^2}}\int\int P(\theta,\phi)\sin(\theta)\mathrm{d}\theta\ \mathrm{d}\phi \int_R^\infty e^{-\beta r^2} r^2 \mathrm{d}r \tag{7}$$

In this way, the 3-D integral in eq 6 has been rewritten as a product of a 2-D integral on the cavity surface and a 1-D integral in the radial direction. The radial integral can be solved analytically, whereas the angular one is well suited for the BEM approach commonly employed within the PCM; the integrand on the cavity surface is evaluated at the representative points of the surface.

The radial integral can be written as follows:

$$\int_R^\infty e^{-\beta r^2} r^2 \mathrm{d}r = \frac{1}{2\beta}\left\{ R e^{-\beta R^2} + \sqrt{\frac{\pi}{4\beta}}[1 - erf(\beta^{1/2}R)]\right\} \tag{8}$$

whereas the angular part can be rewritten as an integral over the cavity surface by considering that the surface area element $\mathrm{d}s = R^2\sin(\theta)\mathrm{d}\theta\mathrm{d}\phi$:

$$\int\int P(\theta,\phi)\sin(\theta)\mathrm{d}\theta\ \mathrm{d}\phi = \frac{1}{R^2}\int\int P(s)\mathrm{d}s \tag{9}$$

The resulting expression is well suited for a BEM treatment since it involves the computation of a quantity over the molecular cavity surface. The problem can then easily be recasted into a BEM form:

$$n_{out} = \sum_i P(s_i) f(s_i) \tag{10}$$

where the sum runs on the number of surface elements (called "tesserae") into which the whole surface has been partitioned and s_i are the corresponding representative points. $P(s_i)$ is the electronic density at such points, and $f(s_i)$ is a weight which is obtained as follows:

$$f(s_i) = \frac{a_i}{2\beta R_i^2 e^{-\beta R_i^2}}\left\{ R_i e^{-\beta R_i^2} + \sqrt{\frac{\pi}{4\beta}}[1 - erf(\beta^{1/2}R_i)]\right\} \tag{11}$$

where a_i is the area of each tessera and R_i is the radius of the sphere where the tessera i belongs. Equation 10 can be interpreted considering that the number of outlying electrons is assumed to be locally proportional to the density at the surface multiplied by the corresponding weight. Here it is necessary to say that the extension of eq 7, which is strictly valid only for a spherical cavity to eq 10 for a cavity made of interlocking spheres, is not rigorous, and its validity has been tested numerically against the old repulsion model. The results are reported in the Appendix. Equation 10 can then be used to generalize the repulsion free energy expression given in eq 3 for a solvent density, $\rho_B(r)$, which depends on the position since we have now associated a fraction of the outlying electrons with the corresponding tessera, namely

$$G_{rep} = \sum_i \alpha' \rho_B(s_i) P(s_i) f(s_i) \tag{12}$$

where $\alpha' = 0.063\ n_{val}^B/M_B$. By making use of the delta function operator, δ_i, one can further write

$$G_{rep} = \sum_i \alpha' \rho_M(s_i) f(s_i)\, tr\boldsymbol{P}\boldsymbol{\delta_i} = tr\boldsymbol{P}\boldsymbol{h}_{rep} \tag{13}$$

The functional derivative of G_{rep} with respect to the density defines the repulsion operator, namely

$$h_{rep} = \frac{\delta G_{rep}}{\delta \boldsymbol{P}} = \sum_i \alpha' \rho_M(s_i) f(s_i) \delta_i \tag{14}$$

Equations 13 and 14 define the repulsion free energy and the corresponding quantum mechanical operator for a solvent density, which is not constant in space, but it smoothly varies

and they can thus be used to study general molecular solutes in the presence of planar interfaces of arbitrary profile.

3. Solvation Energy and Electric Properties of at the Water−Air Interface

3.1. Computational Details. The structure of N_3^- has been optimized in water at the B3LYP/6-31++G* level of theory. The cavity is made of three interlocking spheres of equal radius $R = 1.92$ Å and centered on each nitrogen nucleus. The ion belongs to the $D_{\infty h}$ symmetry group, and the geometry optimization in water solution (dielectric constant $\epsilon = 78.39$) yields a value of 1.187 Å. This structure has been used throughout all the calculations carried out in the present paper. Due to the strength of the N−N bonds, the structure is very rigid and only a negligible change is observed optimizing the geometry in the gas phase, where the bond length is only 0.003 Å longer. In fact, the use of a larger basis set (6-311++G*) yields a variation of 0.006 Å in the bond length. For these reasons, the B3LYP/6-31++G* solvent-optimized molecular geometry has been employed throughout the paper.

As done in the previous study on halides,[22] we have calculated the solvation energy profile, the dipole moment, and the polarizability in order to correlate the surfactant behavior with the variations of the molecular properties at the interface. Moreover, since N_3^- does not have spherical symmetry, we have, in this case, also investigated the orientational dependence by performing the calculations in three different orientations with respect to the planar interface. By taking into account the angle θ between the normal to the surface and the molecular axis, we have performed three different sets of calculations, respectively, with $\theta = 0°$, $\theta = 45°$, and $\theta = 90°$. All the results have been obtained at the density functional theory using the B3LYP hybrid functional and the double-augmented correlation-consistent triple valence basis set of Dunning (daug-cc-pVTZ).[33] This basis set has been chosen as a good compromise between a sufficiently accurate description of the polarization and diffuse character of the wave function and the need for stability and reasonable speed of the calculations. In fact, it has not been possible to use the basis set of Hattig and Hess[34] employed in the previous study[22] because of arising linear dependencies in the basis, whereas passing from the daug-cc-pVTZ basis to, for example, the daug-cc-pVQZ and daug-cc-pV5Z bases did not change substantially the quality of the results but affected significantly the computational costs.

In the following, the static polarizabilities of N_3^- in the gas phase and in bulk water will be briefly discussed, then the results at the interface obtained for the three different orientations will be presented separately, and finally, they will be discussed and compared. The calculations have always been carried out both with the model containing only the solute−solvent electrostatic interaction and with the model containing the electrostatic and repulsion interactions together. For the sake of brevity, from now on, we will respectively refer to them as the "electrostatic model" and the "repulsive model".

All the calculations have been performed using Gaussian 03.[35]

3.2. Static Polarizabilities of N_3^- in the Gas Phase and Bulk Water. In Table 1, we have collected the components and the trace of the static polarizability of N_3^- in the gas phase and in water with the two solvation models. It can be seen that there is a strong solvation effect on the axial component of the polarizability (α_{zz}) which increases substantially, whereas the two perpendicular components ($\alpha_{xx} = \alpha_{yy}$) are much less affected. The comparison of the two different solvation models, with and without repulsion, shows that the effect of repulsion in bulk solution is to reduce the polarizability. This is due to the nature of the repulsive interaction which yields a compression of the electronic density causing the reduction of the polarizability.

TABLE 1: Components of the Static Polarizability Tensor of N_3^- in the Gas Phase and in Water Solution[a]

molecule	in vacuo	IEF−PCM (electrostatic)	IEF−PCM (el+rep)
α_{xx}	30.91	31.38	30.78
α_{zz}	69.88	87.12	85.58
α_{tot}	43.90	49.96	49.05

[a] All values are in arb units and are obtained at the B3LYP/daug-cc-pVTZ level. The values in solution are calculated both with and without repulsion. $\alpha_{yy} = \alpha_{xx}$ and $\alpha_{tot} = 1/3(\alpha_{xx} + \alpha_{yy} + \alpha_{zz})$.

3.3. $\theta = 0°$: N_3^- Perpendicular to the Interface. In Figure 2a, we have collected the solvation energy profiles of N_3^- for $\theta = 0°$ in the case of the electrostatic model and in the case of the repulsive model. Negative values ($z < 0$) correspond to the molecule being immersed in the water phase, whereas positive values correspond to the molecule in the gas phase. The origin is posed at the Gibbs' dividing surface of the dielectric permittivity, $\epsilon(z)$, and the molecule is made to cross the interface from negative values (water phase) to positive values (gas phase).

The solvation energy at a distance of −13 Å from the interface is −59.32 kcal/mol for the calculation with repulsion and −63.31 kcal/mol for the electrostatic model; therefore, the inclusion of repulsion lowers the solvation energy by almost 4.0 kcal/mol. These values can be considered as bulk solvation energies. The electrostatic solvation energy profile is monotone, and the solvation energy gradually increases from its bulk value to zero in the gas phase; around $z = 0$ Å, the profile increases almost linearly, then the classical behavior of a point charge close to a sharp planar interface is recovered and the curve is then proportional to $1/z$.

With the repulsive model, the solvation energy first increases slightly (this feature is evidenced only in the concentration profile shown in Figure 5) similar to the electrostatic one until around $z = -7$ Å, then it decreases and a minimum is observed at $z = -2.75$ Å. The depth of such minimum with respect to the corresponding bulk value is −0.65 kcal/mol, which is comparable to that previously obtained for Cl^- [22] (0.7 kcal/mol). Beyond the minimum, the repulsive profile has features similar to those of the electrostatic one with a nearly linear zone around $z = 0$ Å and a $1/z$ shape in the gas phase.

The presence of the interface induces a dipole moment d_z along the z direction. The induced dipole moment at the interface is shown in Figure 3a; $d_z(z)$ has a maximum at $z = 2.5$ Å for both models. When repulsion is present, a minimum at $z = -3.0$ Å is also present. The value of the dipole moment at the maximum is 2.3 D for the electrostatic model and 2.2 D for the repulsive model. The other two components of the dipole moment are zero by symmetry.

The trace of the polarizability tensor is reported in Figure 4. In bulk water, the polarizability is higher for the electrostatic model since the repulsive interaction causes a compression and thus a "hardening" of the electronic density. In the electrostatic model, the polarizability decreases steadily at the interface, passing through a minimum, and then increases again toward the gas-phase value. In the repulsive model, a small maximum at around −2.5 Å is also observed. After such a maximum, the repulsive model behaves like the electrostatic one, and the two curves are almost overlapped when the minimum is reached.

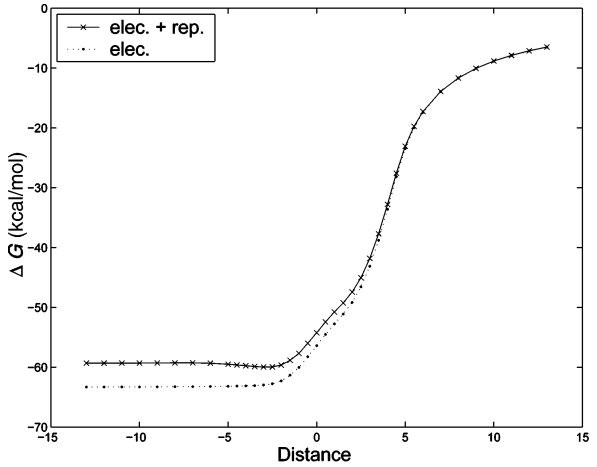

(a) $\theta = 0°$

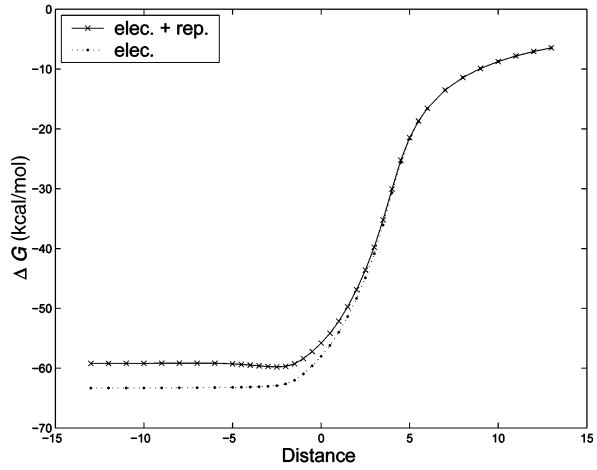

(b) $\theta = 45°$

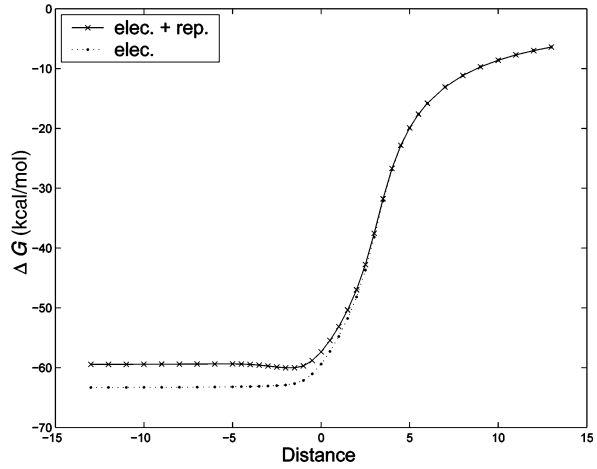

(c) $\theta = 90°$

Figure 2. Solvation energy of crossing the water/air surface in the three selected orientations for the two solvation models: electrostatic (dotted line) and repulsive (continuous line). Distances are in angstroms and solvation free energies in kcal/mol.

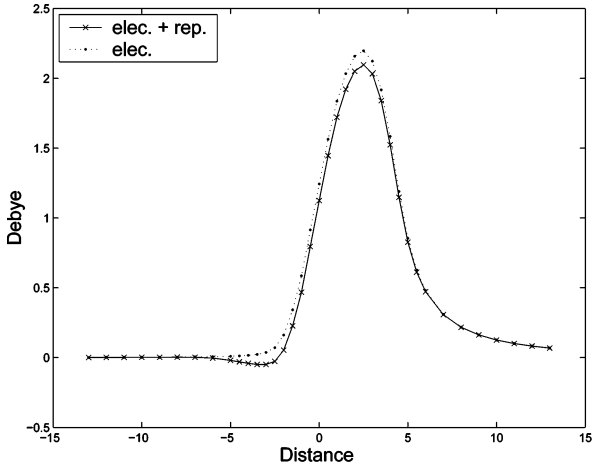

(a) $\theta = 0°$

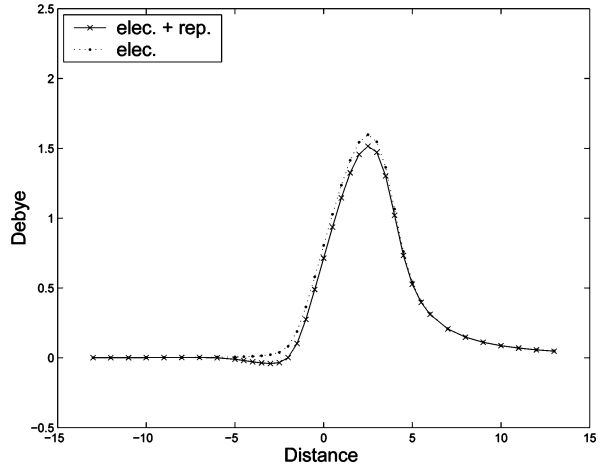

(b) $\theta = 45°$

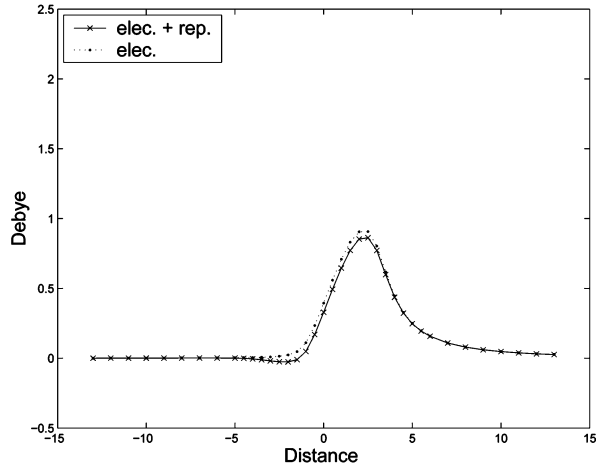

(c) $\theta = 90°$

Figure 3. Dipole moment (z component) of N_3^- crossing the water/air surface in the three selected orientations for the two solvation models: electrostatic (dotted line) and repulsive (continuous line). Distances are in angstroms and dipoles are in Debye.

3.3.1. $\theta = 45°$. We have collected the data for the molecule crossing the interface with an angle $\theta = 45°$. The energy profiles are displayed in Figure 2b, the dipole moments in Figure 3b, and the total polarizabilities in Figure 4b. The results are very similar to those obtained for $\theta = 0°$; therefore, we will limit ourselves to a few remarks. The solvation energy, including repulsion, has a minimum around $z = -2.5$ Å, and its depth, compared to the bulk solvation energy, is about 0.60 kcal/mol. The dipole moment induced by the surface peaks at 2.5 Å with a value around 1.7 D for the total dipole in the repulsive model (the d_z component has a value around 1.5 D at its maximum).

Apart from a small difference in magnitude, the only noticeable difference between the two models is the small side peak for the repulsion model, as observed for $\theta = 0°$. We remark that, for the present orientation, the dipole moment is not

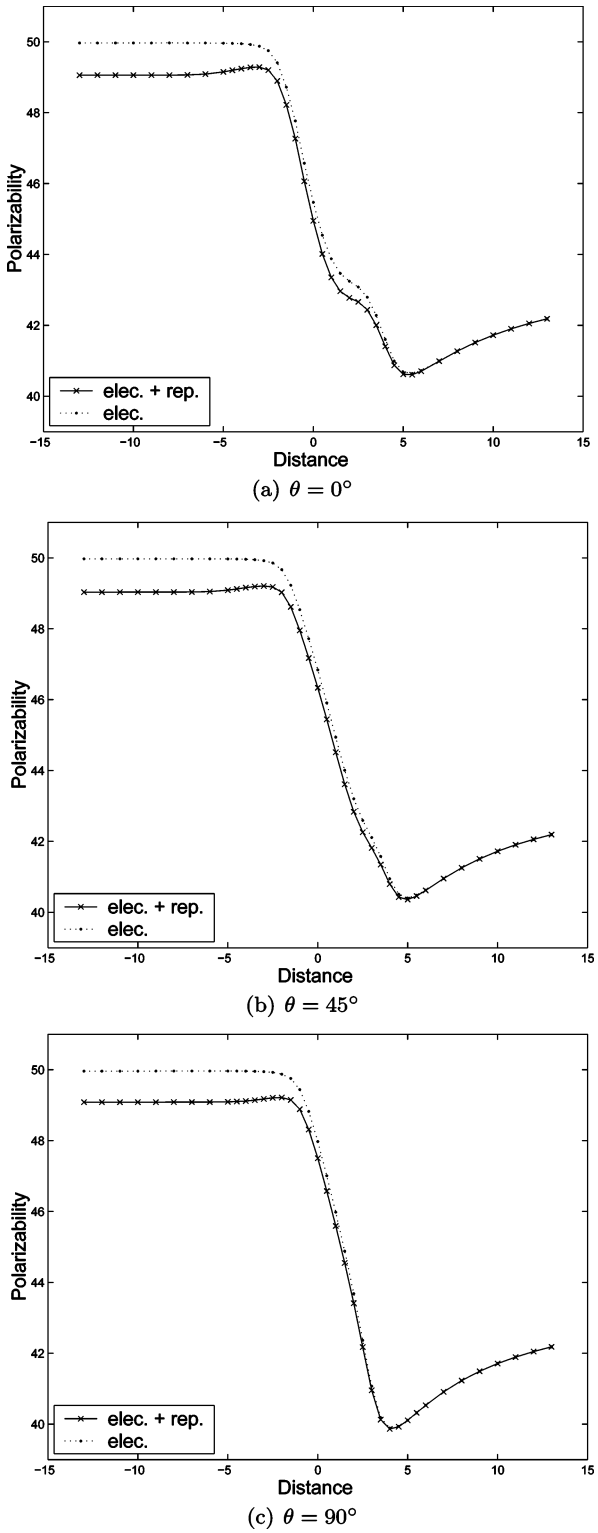

Figure 4. Trace of the polarizability tensor of N_3^- crossing the water/air surface in the three selected orientations for the two solvation models: electrostatic (dotted line) and repulsive (continuous line). Distances are in angstroms and polarizabilities are in arb units.

perpendicular to the interface, but it also has a d_y component parallel to the interface, due to the overall C_s symmetry of the system in this orientation. The d_y component of the dipole moment shows the same behavior at the interface but is smaller in magnitude, thus it has not been shown. Its value at the maximum is around 0.8 D.

The polarizability also has a similar behavior to the previous orientation ($\theta = 0°$), although we notice that the variation of the polarizability across the interface is steeper, and the structure around $z = 0$ has almost disappeared.

3.3.2. $\theta = 90°$: N_3^- Parallel to the Interface. Concerning the third orientation ($\theta = 90°$) corresponding parallel to the surface, the energy profiles are shown in Figure 2c, the dipole moment is shown in Figure 3c, and the polarizability in Figure 4c. As for the previous case ($\theta = 45°$), only a few remarks are necessary in order to highlight the differences with the two other orientations.

The shape of the profiles is similar to the previously investigated orientations. The solvation profile displays a minimum at $z = -1.5$ Å, the depth of the minimum with respect to the bulk value is 0.58 kcal/mol, which is slightly smaller than that in the two other orientations.

The dipole moment induced by the interface is, in this case, perpendicular to the molecular axis since the molecule is oriented along the *y* direction. The induced dipole peaks around $z = 2.5$ Å for both models (with and without repulsion). For the repulsive model, the small minimum at $z = -2.0$ Å is present here, as well. The dipole moment value at its maximum is around 0.8 D for both models.

The polarizability profiles are again similar in the main features to the two other orientations. The profiles are steeper due to the sudden variation of the dielectric properties experienced by the molecule, which is now along the interface and thus is "probing" only a limited portion of the interface at each position.

3.4. Discussion. The presence of the interface induces significant modifications to the molecular electronic density of N_3^-; the anisotropy of the environment induces a displacement of the electronic density with respect to the nuclear positions. This is, for instance, evidenced by the rise of a surface-induced dipole moment which is present for all the investigated orientations. As was the case for the halides,[22] such a charge displacement is strongly correlated with the reduction of the polarizability at the interface, which presents a minimum close to the maximum in the dipole moment. It is easy to understand this correlation: the interface polarizes the molecule, and therefore a dipole moment arises; on the other hand, when the molecule is polarized, the electronic density is stretched with respect to its equilibrium position, and a further polarization is less favorable; therefore its polarizability is reduced. This is a pure electrostatic effect as can be seen by comparing for each figure the two solvation models, the electrostatic and the repulsive one, which both show the same behavior in this respect. The effect of the repulsion contribution can be seen before the electrostatic effect arises: when the molecule is immersed in the water phase but close to the interface, the energy profile has a small energy minimum which is not present in the electrostatic model. By looking at the position of the minimum, we can see that it is closely related to the small minimum for the dipole moment and to the corresponding maximum in the polarizability. The origin of this feature can be rationalized as follows: when the molecule approaches the interface, the repulsion contribution, which is very short-ranged due to its exponential decay, is reduced, whereas the electrostatic one, which is subject to saturation, can still be considered to be as in bulk solution. Since this reduction is anisotropic, the electronic density is free to expand only on one side but not on the other. This explains both the small minimum in the dipole moment (the electrons are, in fact, displaced with respect to the nuclei) and the small maximum in the polarizability, which is caused by the expanded electronic cloud. This effect is soon overcome by the far larger electrostatic effect which causes the

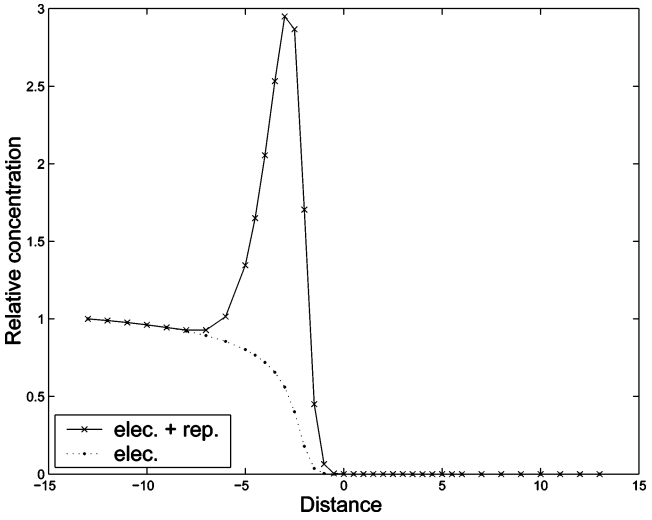

Figure 5. Concentration profiles at the interface obtained by applying the Boltzmann distribution to the calculated free energies. The bulk solvation energy is taken as reference, and the bulk concentration is assumed to be unitary.

inversion of the dipole moment and the reduction of the polarizability. Although the repulsion effect may seem very small, it is worth looking at the results in a different perspective: by assuming that the obtained energy profile could be reflected in the concentration of the species at the interface, one can estimate the interfacial concentration by the Boltzmann distribution. The concentration profile for a bulk concentration, c_0, taking the asymptotic solvation free energy $G_0 = G(-\infty)$ as the reference energy, can be obtained as

$$c(z) = c_0 e^{(G_0 - G(z))/RT} \tag{15}$$

The obtained profile for $\theta = 0°$, assuming a temperature $T = 300$ K and a concentration $c_0 = 1$, is shown in Figure 5. As can be seen, the small correction due to repulsion induces a profound change in the concentration profile at the interface: no such maximum is present for the electrostatic model, which is indeed coherent with the classical picture of ions repelled by the interface. One must anyway bear in mind that such a concentration profile is valid under the assumption of infinite dilution and in the absence of any counterion. Therefore, any cooperative effect that may arise in the presence of the counterion and at finite concentrations is completely neglected.

The comparison of the three different orientations shows that the configuration with $\theta = 0°$ is slightly more favored in energy, although the differences are extremely small (<0.1). The most noticeable difference among the three orientations is the width of the variations at the interface, which is well correlated to length of the molecule along the direction perpendicular to the interface. For instance, taking into account the distance between the maximum and the minimum in the polarizability, we pass from 8 Å for $\theta = 0°$ to less than 7 Å for $\theta = 90°$.

The interfacial solvation of N_3^- has been previously investigated through MD simulations by Yang[23] and subsequently probed experimentally by Petersen and Saykally.[36] Our study agrees with the main experimental finding that N_3^- displays a surfactant behavior, although we are not able to reproduce the significant adsorption free energy of -9.9 kcal/mol obtained by the fitting of SHG measurements. On the other hand, the agreement with MD simulations is remarkable: by comparing our concentration profile obtained applying eq 15 to the density profile shown in Figure 7 of ref 23, we can see that the peak concentration obtained by the MD simulations (45 arb units) is roughly 3−4 times the corresponding bulk value (10−15 arb units). Our model yields a concentration enhancement which is around 3-fold.

In this comparison, however, we cannot forget to say that the present formulation lacks two significant energy contributions (dispersion and cavitation) that could—in principle—affect the current results. On the other hand, it has already been shown that dispersion and cavitation contributions, when they are introduced through an empirical model based on atomic forces,[20] are of opposite sign and almost cancel each other. In particular, if we apply such an empirical model to N_3^-, we obtain a bulk cavitation contribution in water of 7.18 kcal/mol and a dispersion term of -6.73 kcal/mol. The bulk repulsion energy within the current quantum mechanical model is 3.95 kcal/mol, instead. This indicates that the nonelectrostatic contribution to the solvation energy is mainly of repulsive nature. One may argue that the range of variation of dispersion and cavitation energies at the interface may not yield such a close mutual cancellation; however, since dispersion is certainly longer ranged than cavitation, this would reinforce the observed picture of a minimum at the interface. We can then safely conclude that the qualitative picture obtained, including electrostatic and repulsive contributions but not cavitation and dispersion, would not be altered as soon as these latter will be included, although the figures could be slightly different.

4. Summary

In the present work, we have developed and implemented an expression for the repulsion contribution to the solvation energy within the framework of continuum models. The current development was necessary in order to obtain an expression which could be employed in the presence of a nonhomogeneous solvation environment, namely, an interface between two different dielectrics.

The current development is based on the definition of a molecular cavity, and it employs a modeling of the outlying electron density in order to locally describe the solute−solvent repulsion interaction. Although the current formulation is not fully rigorous, it represents an important improvement with respect to the previous one, which was a simple heuristic adaptation of the formulation developed by Amovilli and Mennucci[32] for a homogeneous dielectric. In other words, whereas the previous expression was limited to simple solutes (of spherical symmetry) and thus yielded unphysical results for arbitrary polyatomic systems, the new one is defined in a robust way in this respect, and it can be applied to any molecular solute. Such a new formulation, however, is still an approximated model. The two main approximations introduced are the explicit modeling of the electron density outside the cavity and the reduction of the volume integration to a surface integral estimated in a BEM fashion.

The new repulsion formulation has been coupled to the IEF−PCM electrostatic model and applied to the study of N_3^- at the air−water interface. It has been shown that such an ion displays a pattern similar to that of the halides when its solvation energy, dipole moment, and polarizability are calculated in the presence of an interface. Since the molecule is linear, the orientational dependence has also been investigated by computing the profiles for three different ion−surface orientations. All three profiles show very similar results, although in the perpendicular orientation ($\theta = 0°$), the features are somewhat wider and more marked due to the higher environmental anisotropy experienced by the ion in such an orientation.

TABLE 2: Comparison of the Original and the New Repulsion Models: SCF Energies at the B3LYP/daug-cc-pVDZ in Water Solution Including Repulsion for Fluoride, Water, Formaldehyde, and Methanol[a]

molecule	new model	original model	Δ
F^-	−100.002646	−100.002697	5.1e-05
H_2O	−76.454517	−76.454553	3.6e-05
H_2CO	−114.524905	−114.524941	3.5e-05
CH_3OH	−115.749605	−115.749638	3.3e-05

[a] Geometries were optimized in solution at the same level of theory. The first column is the SCF energy with the new repulsion model; the second one is the same quantity with the old model. The third column collects the observed differences. All values are in Hartree.

The results are in agreement with the experimental findings which attribute a surfactant behavior to N_3^- (as is the case for the halides), and they also agree well with MD simulations performed on the same system. We underline how a small modification to the Hamiltonian as the one introduced by the presence of the repulsion contribution can yield a dramatic change in the system behavior. This is well illustrated by the concentration profile obtained with the two models. The monotonic decay at the interface shown by the electrostatic model, which is in agreement with predictions based on classical electrostatics, is replaced by a significant enhancement of the concentration at the interface which is entirely due to the introduction of the repulsion energy contribution and the fact that this energy term is much more short-ranged than the electrostatic interaction.

The current model shall be further developed by introducing other sources of energy contributions, such as the solute−solvent dispersion interaction, which has currently been neglected. As we have discussed above, the inclusion of dispersion forces should not modify the observed picture of a surfactant behavior for N_3^-, but it should rather reinforce it. Moreover, we would like to underline that, within this approach, it is possible to isolate and understand the effect of each interaction (electrostatics, repulsion, and, in the future, dispersion) separately, thus providing unique insight to the surface solvation. Moreover, the present model makes it possible to treat the molecular system within the very same framework in the gas phase, at the interface, and in bulk solution, thus providing a unique tool to compare the behavior of the investigated molecular species in these three different surrounding environments.

Appendix: A Comparison between the New and the Original Repulsion Model

We present here a direct comparison between the new formulation for repulsion interaction and the original one. For bulk calculations, in fact, the two formulations should, in principle, yield the same results. It is worth recalling here that the original model makes use of the Gauss theorem to obtain an expression of the repulsion Hamiltonian, whereas the new model assumes a Gaussian decay of the molecular density starting from its value at the surface. The number of outlying electrons is employed to determine the coefficient β of the Gaussian function, then the repulsion contribution is evaluated directly. On one hand, this allows for the extension to the interface since the obtained expression can be naturally extended to the case of a nonconstant solvent density. On the other hand, the assumption of a Gaussian decay is arbitrary, and the equivalence of the two expressions in bulk solution is not exact but must be tested.

The comparison is reported in Table 2, where the SCF energy in water solution with the two repulsive models is shown for a set of small molecules. All calculations have been carried out at the B3LYP/daug-cc-pVTZ level. It can be seen that the variations in the SCF energy are of the order of 10^{-5} Hartree or 10^{-2} kcal/mol. This is negligible in comparison to the absolute values of the repulsive energy term, which is of the order of 1−5 kcal/mol.

References and Notes

(1) Chang, T.-M.; Dang, L. X. *Chem. Rev.* **2006**, ASAP.
(2) Jungwirth, P.; Tobias, D. J. *Chem. Rev.* **2006**, ASAP.
(3) Wagner, C. *Phys. Z.* **1924**, *25*, 474.
(4) Onsager, L.; Samaras, N. N. T. *J. Chem. Phys.* **1934**, *2*, 528.
(5) Jungwirth, P.; Tobias, D. J. *J. Phys. Chem. B* **2000**, *104*, 7702.
(6) Jungwirth, P.; Tobias, D. J. *J. Phys. Chem. B.* **2001**, *105*, 10468.
(7) Salvador, P.; Curtis, J. E.; Tobias, D. J.; Jungwirth, P. *Phys. Chem. Chem. Phys.* **2003**, *5*, 3752.
(8) Brown, E. C.; Mucha, M.; Jungwirth, P.; Tobias, D. J. *J. Phys. Chem. B* **2005**, *109*, 7934.
(9) Dang, L. X.; Chang, T. M. *J. Phys. Chem. B* **2002**, *106*, 235.
(10) Dang, L. X. *J. Phys. Chem. B* **2002**, *106*, 10388.
(11) Dang, L. X. *J. Chem. Phys.* **2003**, *119*, 6351−6353.
(12) Garrett, B. C. *Science* **2004**, *303*, 1146−1147.
(13) Petersen, P. B.; Saykally, R. J. *Chem. Phys. Lett.* **2004**, *397*, 51.
(14) Ghosal, S.; Hemminger, J. C.; Bluhm, H.; Mun, B. S.; Hebenstreit, E. L. D.; Ketteler, G.; Ogletree, D. F.; Requejo, F. G.; Salmeron, M. *Science* **2005**, *307*, 563.
(15) Gopalakrishnan, S.; Jungwirth, P.; Tobias, D. J.; Allen, H. C. *J. Phys. Chem. B* **2005**, *109*, 8861−8872.
(16) Cancès, E.; Mennucci, B.; Tomasi, J. *J. Chem. Phys.* **1997**, *107*, 3032.
(17) Cancès, E.; Mennucci, B. *J. Math. Chem.* **1998**, *23*, 309.
(18) Mennucci, B.; Cammi, R.; Tomasi, J. *J. Chem. Phys.* **1998**, *109*, 2798.
(19) Miertus, S.; Scrocco, E.; Tomasi, J. *Chem. Phys.* **1981**, *55*, 117.
(20) Frediani, L.; Pomelli, C. S.; Tomasi, J. *Phys. Chem. Chem. Phys.* **2000**, *2*, 4876.
(21) Frediani, L.; Cammi, R.; Corni, S.; Tomasi, J. *J. Chem. Phys.* **2004**, *120*, 3893.
(22) Frediani, L.; Mennucci, B.; Cammi, R. *J. Phys. Chem. B* **2004**, *108*, 13796.
(23) Yang, X.; Kiran, B.; Wang, X. B.; Wang, L. S.; Mucha, M.; Jungwirth, P. *J. Phys. Chem. A* **2004**, *108*, 7820.
(24) Tomasi, J.; Persico, M. *Chem. Rev.* **1994**, *94*, 2027.
(25) Tomasi, J.; Mennucci, B.; Cammi, R. *Chem. Rev.* **2005**, *105*, 2999.
(26) Onsager, L. *J. Am. Chem. Soc.* **1936**, *58*, 1486.
(27) Clay, J. R.; Goel, N. S.; Buff, F. P. *J. Chem. Phys.* **1972**, *56*, 4245.
(28) Perram, J. W.; Barber, M. N. *Mol. Phys.* **1974**, *28*, 131.
(29) Stern, F. *Phys. Rev. B* **1978**, *17*, 5009.
(30) Amovilli, C. *Chem. Phys. Lett.* **1994**, *229*, 244.
(31) Amovilli, C.; Mcweeny, R. *Chem. Phys.* **1990**, *140*, 343.
(32) Amovilli, C.; Mennucci, B. *J. Phys. Chem. B* **1997**, *101*, 1051.
(33) Kendall, R.; Dunning, T.; Harrison, R. *J. Chem. Phys.* **1992**, *96*, 1992.
(34) Hattig, C.; Hess, B. A. *J. Chem. Phys.* **1998**, *108*, 3863.
(35) Frisch, M. J.; et al. *Gaussian 03*, revision B.03; Gaussian, Inc.: Pittsburgh, PA, 2003.
(36) Petersen, P. B.; Saykally, R. J.; Mucha, M.; Jungwirth, P. *J. Phys. Chem. B* **2005**, *109*, 10915.